Bulletin of Glacier Research 7 (1989) 7–14

Ice thickness and subglacial topography obtained by radar sounding on Chongce Ice Cap, West Kunlun Mountains.

ZHU Guocai
Lanzhou Institute of Glaciology and Geocryology, Academia Sinica, Lanzhou, China

(Recived December 9, 1988; Revised mamuscript received January 20, 1989)

Abstract

Improved equipment called pulse modulation radar, type B–1, frequency 300 MHz, was used to measure ice thickness on the Chongce Ice Cap as one of the glaciological observations of the Sino–Japanese Joint Expedition on the south slope of the West Kunlun Mountains in June–August 1987. The measurements were made, mainly in the fan–shape area on the ice cap, between 5800 and 6300 m a.s.l., at 1300 points along measurement lines up to 60 km long, covering about 21 km^2 in area. The main results are as follows: the maximum ice thickness was observed to be 214 m at 6100 m a.s.l. on the Guozha Glacier; 151 m at 6000 m. a.s.l. on the Chongce Ice Cap; 66.1 m at 6366 m. a.s.l., at the top of the ice cap. The amount of ice stored in the fan–shape area of the ice cap is 1.286 km^3 with an average thickness of 70.9 m. An equation is proposed to express ice thickness in terms of surface slope, based on the observation: $H=28.6 \tan^{0.6} \alpha$, where H is ice thickness in m and α is surface slope. Subglacier microtopography, consisting of the ditch and dike of the radius and glacier erosion basins, were observed along the transverse observation lines. The longitudinal section, however, is similar to the form of cirque glaciers.

1. Introduction

For over 20 years, the thicknesses of polar ice sheets and mountain glaciers have been measured with the use of radar sounders. This method has the advantage over early methods of gravity and seismic sounding in the both of accuracy and speed, so it has been widely used. This paper describes the ice cap thickness and subglacial topography according to these data.

2. The sounding range and equipment

The West Kunlun Mountains are located west of Qinghai and the boundary between Xinjang and Xizang. The highest peak of the Kunlun Mountains is 7167 m a.s.l., and glaciers around it occupy three–fourths of the total glacier area in the Kunlun Mountains. The Chongce Ice Cap is about 17 km south–east of Kunlun Peak. The Guozha Glacier is to the west, and the Chongce Glacier to the east of it. Figure 1 shows the fan–shaped area of the ice cap, where the radar sounding was carried out, 18.135 km^2 in area (Chen *et al.*, 1988). The total area covered by the sounding was about 21 km^2.

The measuring equipment is a glacier radar, type B–1, shown in Fig. 2. It was made in 1982, and improved to be suitable for continental glaciers. It can be operated by 3 persons. Its basic system and principle have been described by Zhu (1982). An improved version of the system with 3Ah battery can be used continuously for about 120 minutes, allowing measurements of about 150 points to be made. In order to recognize the records, a new five–digit LED numerical display was set on the system; with it one can distinguish the location of the measuring point. This number was recorded on the same photograph as the record of reflected waves.

The specifications of the radar system are as

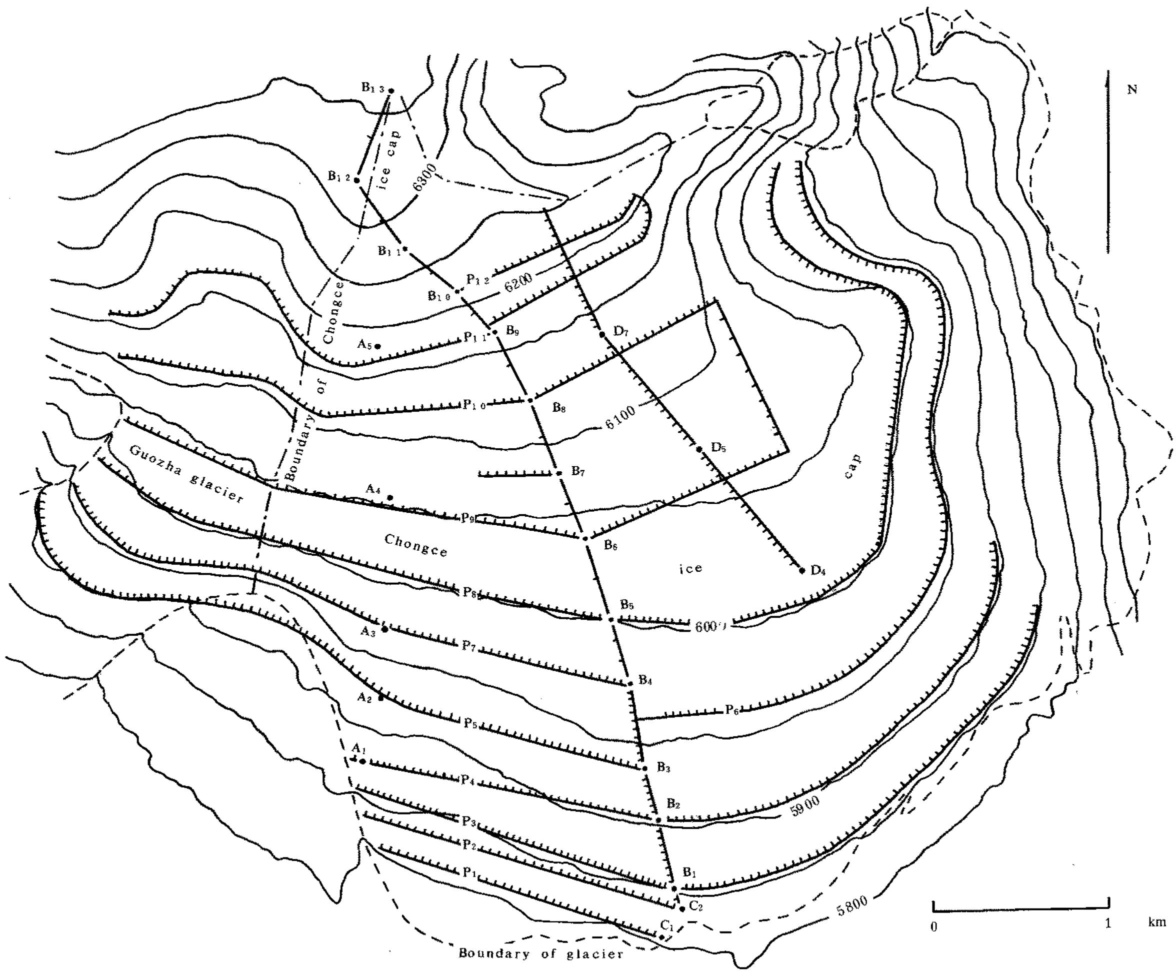

Fig. 1. Lines of radar sounding on the Chongce Ice Cap.

follows: carrier frequency 300 MHz, modulation pulse widths: 50 ns and 150 ns, duplication period 2 s and 5 s, middle frequency of receiver 50 MHz, radar−echo display middle frequency, emission power 1−5W, receiving and emitting antenna a plane−spiral antenna with reflecting screen of 10 dB gain, total gain 130 dB, maximum ice thickness about 400 m, thickness resolving power 1 m (2 s) and 2.5 m (5 s), power supply 12 Cd−Ni storage batteries (3 Ah each) chargeable by solar energy, total weight 18 kg.

The measurement accuracy was checked with an actual measurement of ice thickness by a drilling down to the bed rock on the No. 1 Glacier, Urumqi river basin. Relative error was within 5% (Zhang *et al.*, 1985).

3. Field work

The position of each measurement was determined with reference to a stake network surveyed on the ice cap (Chen *et al.*, 1989). The measurements were made along contour lines as shown in Fig. 1, using a step−measurement method. The height difference between measuring lines was 50 m, the upper line being at 6200 m a.s.l. There were 11 lines in the west and 9 lines in the east (from P1 to P12) in addition to two longitudinal lines. Detailed studies were carried out around stake B13 on top of the ice cap. The total length of the measurements was over 60 km, which corresponded to 1300 points. The area covered reached 80 % of the ice cap.

The receiving and emitting parts were set 10 m apart. It took only one minute to measure the thick-

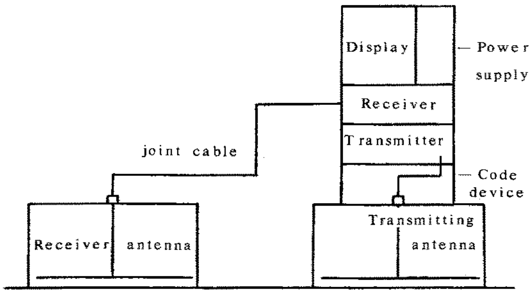

Fig. 2a. Diagram of the improved version of type B−1 radar.

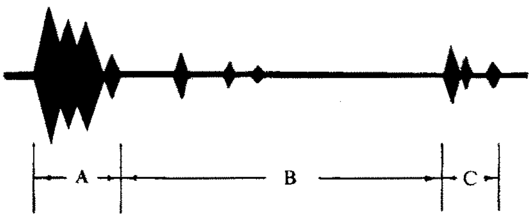

Fig. 2b. Waveform of radar−echo.

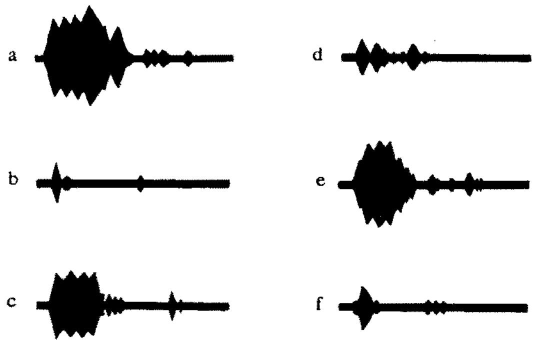

Fig. 3. Radar−echo photographies.

ness at one point. On some occasions, when the weather was fine and surface ablation was intense, melt water percolated into snow layers, and the radar signal was absorbed and attenuated significantly so that the echo record was too small to distinguish. Above 6200 m a.s.l., because of non−uniformity of the surface layer including thin ice bodies in the snow layer, multiple echoes were observed. Adjustment of the position and height of antennas allowed estimation of the echo from the bed. The ice thickness was obtained at 93% of the measurement points.

The form of each echo gave information on ice surface, interior ice and ice at the base. Figure 2 shows that a radar−echo can be divided into three ranges, A, B and C. Range A indicates the surface and the surface layer. Because the surface and the surface layer consist of air, new snow, wet snow, firn, water and ice of different electrical conductivity, the width of range A appeared to be larger than it should be. Although the A−range thickness could not be analyzed quantitatively, we can obtain the relative thickness and detailed structure of the surface layer at various locations on the ice cap. For example, the large and wide A−wave in the accumulation area far above 6200 m. a.s.l. is the result of non−uniformity of the surface layer (Fig. 3a), which was found in the ice core (Han *et al.*, 1989). Near the bare ice surface below 5900 m. a.s.l., the A−wave is small in both amplitude and tail, and the base echo was large; it shows a thin and simple surface layer (Fig. 3b). Between 5900 and 6200 m. a.s.l., the A−wave increased with increasing elevation, which indicated that the surface layer became thin gradually. The thickness of the surface layer was estimated to be 30−35 m at 6200 m a.s.l. The B−range contains waves reflected from the ice interior. B−waves in the B−range should reflect the internal condition of the ice cap, *i.e.*, in the middle part of the ice cap above 80 m depth. A number of small interference waves appeared and a non−reflecting wave area (20−60 m) on the base echo was considered to show stable electric properties, with little moraine and weak reflection in this area (Fig. 3c). At the edge of the ice cap, where the ice thickness was less than 50 m, the reflected waves appeared successively in the B−range, possibly indicating englacial moraine content (Fig. 3d). The C−range contains the base echo. A strong and simple C−wave shows that the base is smooth or is strongly reflecting (Fig. 3e). Where the C−wave changes in its intensity, the ice−rock interface could change in slope.

4. Statistical analysis and results

The ice thicknesses are shown for a transverse section (Fig. 4) and a longitudinal section (Fig. 5). Selected data are in Table 1.

1) As shown in Table 2, the average thickness H along a contour line in the fan−shaped area increased with elevation, 5800−6118 m a.s.l., although it fluctuated slightly. The rate of increase is +0.3 m/m of increase in elevation at 5900−6000 m a.s.l., and +0.2 m/m, at 6000−6118 m a.s.l.. The thickness H reached a maximum of about 151 m at around 6000 m a.s.l.. Above this height, the thickness decreased at a rate of 0.4

m/m. These show that the maximum of average thickness appeared near the heighest point on the equilibrium line (Ageta *et al.*, 1989). The maximum thickness in the Guozha Glacier is 214 m at 6100 m a.s.l..

2) Figure 6 shows the thickness isopleth in the measuring area. The thickest area appeared beside B5 at 6000 m. a.s.l.. The thickness was distributed having a center around that point and became thin gradually all around. The isopleths appear to be irregular circles. Table 3 gives the area values of various thickness ranges in the fan–shaped area, from which the total amount of ice storage was calculated to be 1.286 km^3. The average thickness was 70.9 m. As shown in Fig. 5, the slopes of the surface and bedrock are rather small, *i.e.*, 0.06–0.16, and 0.04–0.18 in tangent of the slope angle respectively. The relation between ice thickness and surface slope is given in Table 4. In this table, the surface slope has an average value for a distance larger than 2.6 times of the average ice thickness for that segment. The variation of thickness is less than 12 m in each segment.

An empirical relation between ice thickness and surface slope was found, from Table 4, as follows:

$$H=28.6/\tan^{0.6}\alpha$$

where H is ice thickness in m, and α the dip angle of the ice surface. When $\alpha<10°$, assuming $\tan\alpha\approx\sin\alpha$, our formula becomes equivalent to Nye's ($H=H_0/\sin\alpha$; H_0 is a constant). Our formula is considered suitable for tan α in a range of 0.06–0.16.

Table 1. Ice thickness data along A, B, C and D lines.

No. of points	Thickness (m)	Altitude (m)
A 1	50.4	5875
A 2	89.7	5925
A 3	102.1	5973
A 4	97.0	6055
A 5	58.8	6180
B 1	82.7	5854
B 2	91.5	5902
B 3	107.9	5936
B 4	129.0	5974
B 5	146.2	5997
B 6	121.7	6025
B 7	112.4	6073
B 8	110.4	6118
B 9	100.0	6165
B10	94.5	6213
B11	77.7	6270
B12	67.6	6327
B13	66.1	6366
C 1	21.6	5801
C 2	57.5	5840
D 4	104.3	6014
D 5	129.5	6075
D 7	111.5	6140

Table 3. Distribution of various ice thicknesses.

Thickness (m)	Average thickness (m)	Area (km^2)	Reserves (km^3)
140 — 151	145.5	0.214	0.0311
120 — 140	130	0.794	0.1032
100 — 120	110	4.028	0.4431
80 — 100	90	2.698	0.2428
60 — 80	70	3.100	0.2170
40 — 60	50	2.636	0.1318
<40	25	4.665	0.1166
Total	70.9	18.135	1.286

Table 2. Ice thickness data along P line.

Name of sections	Length (m)	Altitude (m)	No. of point	Thickness (m) Chongce Ice Cap mean	max.	Guozha Glier mean	max.
P 1	1728	5801	36	42.6	75.5		
P 2	1862	5840	39	63.2	86.3		
P 3	4680	5854	105	53.1	94.6		
P 4	4540	5902	97	73.0	110.4		
P 5	4095	5936	92	76.6	118.6	75.9	158
P 6	4950	5955	95	81.3	121.0		
P 7	3426	5974	78	86.3	151.0	99.1	163
P 8	7820	5997	158	93.4	151.0	98.6	159.8
P 9	3988	6025	75	92.6	133.8	102.8	183.4
P10	3540	6118	73	91.3	119.7	120.4	214.0
P11	3700	6165	74	67.8	123.2	96.6	163.2
P12	1250	6213	26	53.6	94.5		

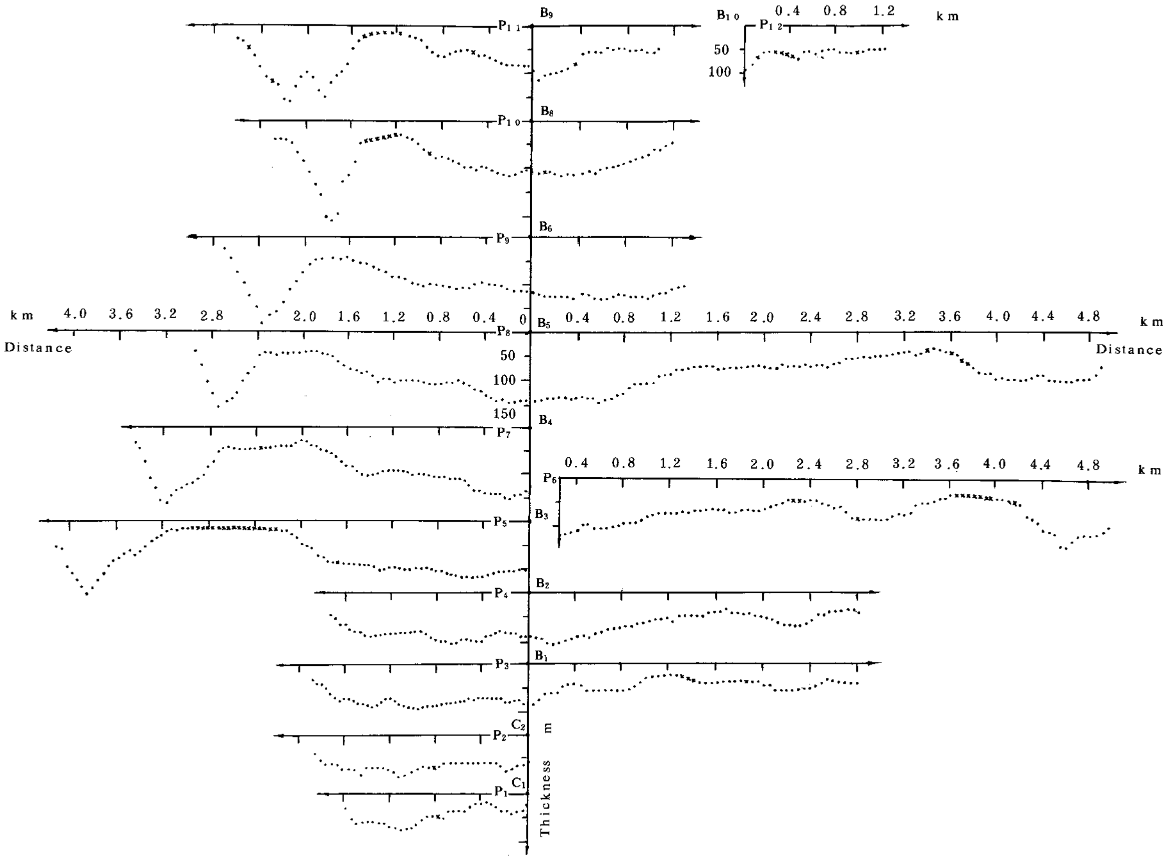

Fig. 4. Cross-section of Chongce Ice Cap.

5. Description of subglacial topography

The topography under the fan-shaped area is rather smooth. The longitudinal and transverse slopes vary uniformly. There are eight smaller ditches and rises and four depressed areas. Figure 7 shows that the lines of ridges and valleys are approximately parallel to the ice flow direction of the ice cap (Chen *et al.*, 1989).

1) Under the effect of original topography and modern ice flow, a lower bed could have been eroded further. Two depressions (L_1, L_2) appear below 6000 m a.s.l. in the east. L_1 has developed an active cirque 2 km long and 0.9 km wide; the maximum thickness 143.8 m appears in the center of the cirque at 5900 m a.s.l. Depression L_2 is eroded and developed slowly because of a smaller amount of ice from upper area, and the maximum thickness of 88 m appears in the center of the depression at 5900 m a.s.l. Discontinuous depressions (L_3, L_4) appear both east and west of stake B5;

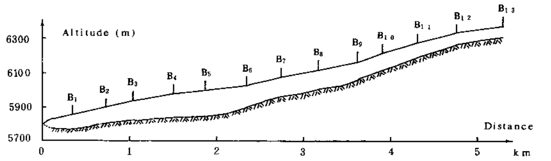

Fig. 5a. Longitudinal section (B1-B13) of the Chongce Ice Cap.

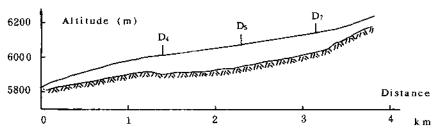

Fig. 5b. Longitudinal section (D4-D7) of the Chongce Ice Cap.

the western one with a maximum thickness of 151 m is larger.

2) There are eight (g_1-g_8) small ridges in the bed. Edge g_1 is the divide of the Guozha Glacier and the ice cap. From north to south, its top is wide and smooth,

and the width of the lower part at 5975 m. a.s.l. is about 600 m and narrows to 250 m at 6050 m a.s.l. upward. The ice layer thickness of the upper part is less than 60 m. Ridge g_2 is wide in the upper part, but narrows with decreasing elevation, and is discontinuous at 6050 m. a.s.l.. The widths of g_3 and g_4 are 50 and 150 m respectively, yet their heights are small. Ridges g_5, g_6 and g_7 are short (1.1 km) and their width is about 150 m. They become lower in height with increasing elevation, and eventually disappear at an elevation of about 6000 m. Ridge g_8 is the northern boundary of the fan–shaped area, extending to expos-

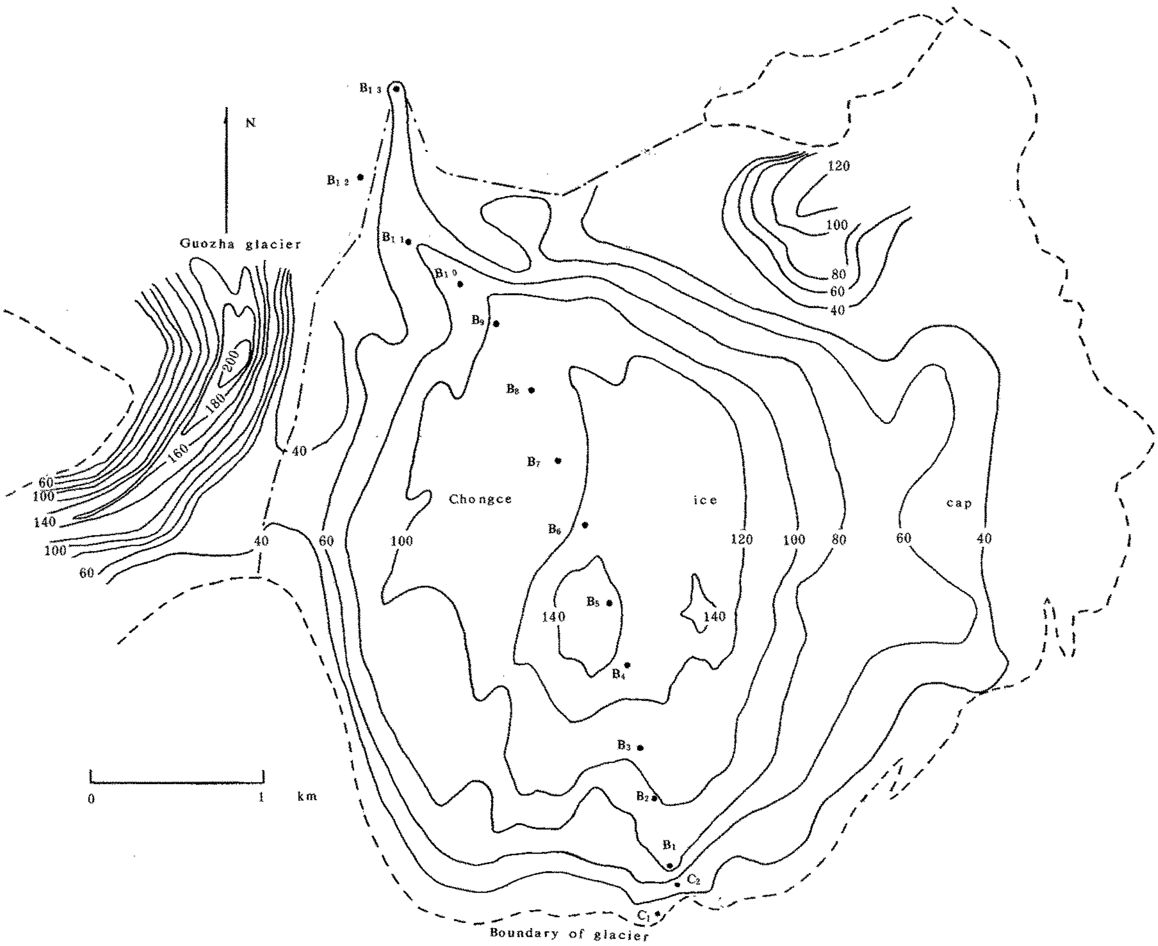

Fig. 6. Isopach of the ice thickness of the Chongce Ice Cap

Table 4. Relation between ice thickness and surface slope. $i=\tan\alpha$

Segment	Starting point	altitude (m)	Terminal	altitude (m)	Distance (m)	Dif. of altitude (m)	slope tan α	Measured average thickness H_0(m)	$H_0 x i^{0.6}$	Calculated average thickness H^*(m)	Relative error (%)
1	B 2	5902	B 3	5936	306.4	34	0.1224	102.3	29.01	100.8	−1.2
2	B 4	5974	B 5	5997	361.3	23	0.0702	139.1	28.27	140.7	+1.2
3	B 7	6073	B 8	6118	429.5	45	0.1064	112.2	29.25	109.7	−2.2
4	B10	6213	B11	6270	400.0	57	0.1516	87.3	28.15	88.7	+1.0

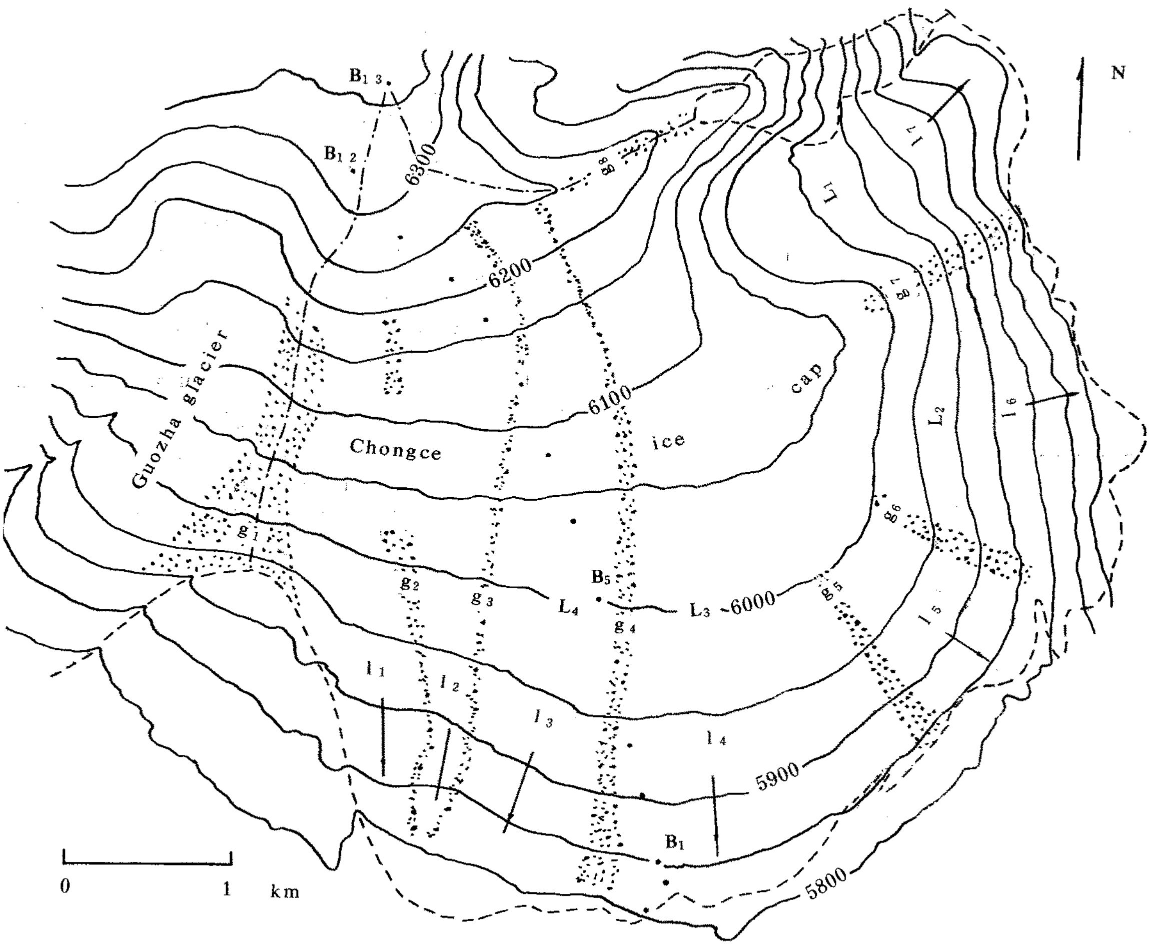

Fig. 7. Subglacial topography of the ice cap.

ed rock at low elevation. The heights of g_2-g_6 in the fan–shaped area are about 20 m. 3) Seven gullies (l_1-l_7) are formed between the eight ridges. Gullies l_1, l_2 and l_3 are rather deep. The ice flow concentrates toward the exit, which is 1.4 km wide. In front of the exit a morainal lake has been formed. The valley l_4 is weaker than the others, probably due to diverging ice flow. In the western part it diverges less than in the eastern part, and the western ice flow is stronger, so in the front of exit a small–scale morainal lake is formed too. There is no morainal lake in front of the eastern part. Valleys l_5 and l_6 have stronger diffusion. Valley l_7 is concentrated ice flow, having features similar to those of a cirque glacier.

Figure 8 shows the ice thickness and surface around the top of the ice cap. We can think that stake B13 is located at the top of the ice cap, and the topography is smooth around 50 m, with a thickness of 60–70 m. In the direction of SW 10°, there is a ridge ten and more meters high through in the east it is 100 m away from stake B12. The angle of the B12 base is about 11.5° toward the southwest. Exposed rock appears 150 m away from B13 in the direction of NW65°; this direction is the ice divide between south and north ice flows.

Acknowledgments

The author is grateful to Dr. Y. Ageta and all team memebers for their help in the field work, and to professors Xie Zichu, Zheng Benxing, Cheng Jianming, Gu Zhongwei, Zhang Wenjing, and Han Jiankang for their help and direction in the analysis.

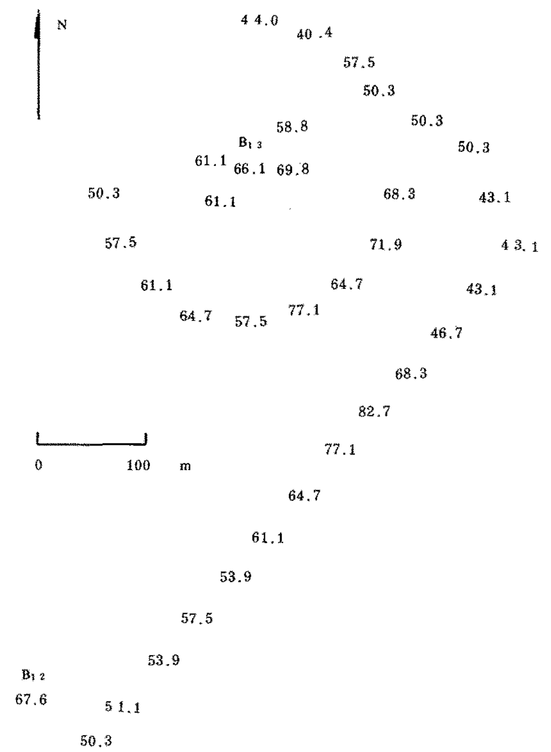

Fig. 8. The ice thickness of the top of the Chongce Ice Cap.

References

Ageta, Y., Zhang, W. and Nakawo, M. (1989): Mass balance studies on Chongce Ice cap in the West Kunlun Mountains. Bulletin of Glacier Research, **7**, 37–43.

Chen, J., Nakawo, M., Ageta, Y. and Watanabe, O. (1989): Movement of Chongce Ice Cap and recent variations of some glaciers on the south side of West Kunlun Mountains. Bulletin of Glacier Research, **7**, 45–48.

Han, J., Zhou, T. and Nakawo, M. (1989): Stratigraphic and structural features of ice cores from Chongce Ice Cap, West Kunlun Mountains. Bulletin of Glacier Research, **7**. 21–28.

Zhu, G. (1982): Type B–1 experimental radar installation for measuring the thickness of glacier. Journal of Glaciology and Cryopedology. **4**, 2, 93–95(in Chinese).

Zhang, X., Zhu, G., Qian, S., Chen, J. and Shen, Y. (1985): Radar measuring ice thickness of No.1 glacier at the source of Urumqi river, Tianshan. Journal of Glaciology and Cryopedology. **7**, 2, 153–162(in Chinese).